Am J Transl Res 2021;13(2):462-479
www.ajtr.org /ISSN:1943-8141/AJTR0124623

*Original Article*

# LncRNA-MALAT1, as a biomarker of neonatal BPD, exacerbates the pathogenesis of BPD by targeting miR-206

Limin Zhang, Xueyan Bai, Wenpeng Yan

*Neonatal Intensive Care Unit, Zhoukou Central Hospital, Zhoukou 466000, Henan, China*

Received October 21, 2020; Accepted November 18, 2020; Epub February 15, 2021; Published February 28, 2021

**Abstract:** Neonatal bronchopulmonary dysplasia (BPD) is one of the common causes of premature birth complications, which is caused by lung dysplasia. Long non-coding RNA (LncRNA) has been proved to be related to BPD and other disease processes, but the molecular mechanism of metastasis-related lung adenocarcinoma transcript 1 (MALAT1) in BPD has not been fully understood. This study focused on exploring the clinical and molecular mechanism of MALAT1 in neonatal BPD, aiming to provide new insights for the management of neonatal BPD. In our study, we first found that serum MALAT1 was up-regulated in neonatal BPD and severe BPD. Further, through receiver operating characteristic curve (ROC) analysis, it was found that the area under the curve of MALAT1 for differentiating neonatal BPD from severe BPD was 0.943 and 0.866, respectively. Then, we established BPD models in vivo and in vitro with C57BL/6J mice and BEAS-2B cells, and found that MALAT1 was also highly expressed in them and increased with the induction time of the models. Pathological evaluation confirmed that down-regulating MALAT1 or up-regulating miR-206 might improve the pathological condition of BPD. Obvious inflammatory response, oxidative stress and up-regulated apoptosis were observed in BPD models in vivo and in vitro. However, after MALAT1 knockdown treatment, the above abnormal phenomena were alleviated to varying degrees. Furthermore, we also found that MALAT1 has a targeted relationship with miR-206, and miR-206 is down-regulated in BPD in vivo and in vitro. Down-regulating miR-206 could also eliminate the anti-BPD effect after knocking down MALAT1. The above results indicated that MALAT1 has the potential as a blood biomarker of neonatal BPD, and MALAT1-miR-206 axis mediates BPD process, which may be a new target for neonatal BPD treatment.

**Keywords:** Newborn, bronchopulmonary dysplasia, LncRNA-MALAT1, miR-206

## Introduction

Bronchopulmonary dysplasia (BPD) is a common complication of premature birth, which poses a serious threat to the survival rate and quality of life of newborns [1]. Its typical feature is impaired alveolar development in neonates, but the specific molecular mechanism has not yet been clarified [2]. It is known that the development of BPD can lead to multiple organ diseases, and this negative effect will affect nearly half of extremely low-birth-weight infants, and it is also related to children's lifelong long-term lung diseases and even abnormal neurological development [3, 4]. Therefore, exploring biomarkers and molecular mechanisms of BPD is of great significance to improve the survival and prognosis of neonatal BPD, and it may provide reference for the diagnosis and treatment of neonatal BPD.

The pathological process of BPD involves inflammation, oxidative stress and apoptosis. On the one hand, the increase of neutrophils and macrophages in the process of inflammatory reaction has a great negative impact on the lung injury caused by neonatal BPD, which will lead to the overactivity of proinflammatory factors, the imbalance of pulmonary proteolytic activity, and the increase of vascular permeability [6]. On the other hand, the threat of oxidative stress to newborns is that it may lead to a series of oxygen free radical diseases, such as retinopathy of prematurity, intraventricular hemorrhage and BPD [7]. Newborns have weak antioxidant defense, and basically have no resis-

tance to the attack of oxygen free radicals. Moreover, oxidative stress can promote inflammatory reaction, further strengthen the secretion of pro-inflammatory factors, damage the respiratory epithelium, and inactivate its surfactant [8, 9]. As for apoptosis, it is an inevitable abnormal manifestation of cells in the progression of BPD. Inhibition of this is helpful to reverse the pulmonary abnormality of neonatal BPD, and plays a certain role in improving endothelial cell function and vascular growth [10].

Long non-coding RNA (LncRNA) is a long-chain RNA molecule, which can reshape chromatin state by acting on chromatin and recruiting protein complexes, thus regulating gene expression [11]. LncRNA has played a regulatory role in many physiological and pathological processes. For example, H19 can promote inflammatory response in the process of BPD by activating MAPK signaling pathway [12]. Another study pointed out that the role of metastasis-related lung adenocarcinoma transcript 1 (MALAT1) in lung inflammation and fibrosis during lung injury was related to the regulation of macrophage activation [13]. In addition, MALAT1 can also regulate the development of BPD disease, and can act on BPD process by targeting miR-129-5p and actively regulating HMGB1 [10]. In this study, we found MALAT1 is involved in another regulatory pathway of BPD pathogenesis, namely MALAT1-miR-206. First of all, we found that the existence of this pathway in infantile hemangioma has certain influence on the proliferation, invasion and migration of endothelial cells [14]. Furthermore, miR-206 was found to improve the development of BPD by targeting the inhibition of fibronectin 1 (FN1).

In this study, we mainly explored the influence of MALAT1-miR-206 axis on inflammation, oxidative stress and apoptosis during the development of BPD, and analyzed the potential of MALAT1 as a biomarker of BPD, hoping to provide new cognition for the management of neonatal BPD.

## Data and methods

### *Serum sample collection*

Forty-five newborns diagnosed with BPD and 40 non-BPD newborns in Zhoukou Central Hospital from December 2015 to December 2019 were selected as BPD group and non-BPD group respectively. The diagnostic criteria were as follows [10]: oxygen therapy was still needed after 36 weeks of gestational age correction; there were typical BPD features in imaging examination, such as enhanced texture, decreased permeability, emphysema, and cystic changes. We excluded all newborns with congenital heart disease, infectious diseases, pneumothorax or other lung diseases. The peripheral blood was collected within 6 hours after birth, and the samples were centrifuged at 1500×g, 4°C for 10 min, and then the serum was collected for subsequent experiments. For BPD group, it was further divided into severe group (n=16) and non-severe group (n=29). The diagnostic criteria for severe group were as follows [16]: newborns who need more than 30% of $O_2$ or continuous positive airway pressure (CPAP)/mechanical ventilation after 36 weeks of gestational age correction. Our research has been approved by the Clinical Ethics Committee of our hospital, and the patients' families have signed informed consent form.

### *Animals*

Altogether 100 newborn C57BL/6J mice (Changsheng Biotechnology Co., Ltd., Benxi, China) weighed 3.82±0.45 g were fed at 25°C with 50% humidity for 12 h light/dark cycle. Our animal experiments were conducted in strict accordance with the guidelines for the care and use of experimental animals, and have been approved by the Animal Ethics Committee of Zhoukou Central hospital.

### *Construction of BPD in vivo model*

In vivo model of BPD was established as described above [17]. Within 12 hours after birth, newborn mice placed in hyperoxia (85% $O_2$) were taken as Ctrl group (n=50) and mice placed in indoor air (21% $O_2$) were taken as BPD group (n=50) for 7 consecutive days. The peritoneum of these two groups of mice were injected subcutaneously with si-NC and MALAT1 inhibitory sequence, miR-NC and miR-206 mimetic, and the same amount of normal saline (0.9% NaCl). Then, they were randomly divided into Ctrl group, Ctrl+si-NC group, Ctrl+si-MALAT1 group, Ctrl+miR-NC group, Ctrl+miR-206 group, BPD group, BPD+si-NC group, BPD+si-MALAT1 group, BPD+miR-NC group and BPD+miR-206 group. The mice were euthanized by

intraperitoneal injection of 5% pentobarbital sodium. The chest was opened and bled by endotracheal intubation, and the lung tissue was removed quickly. Then the left lung was sliced and fixed, and the right lung was frozen in liquid nitrogen and placed in a refrigerator at -80°C for later use.

In addition, according to the previous research method [18], it was also necessary to detect the mean linear intercept (MLI), radial bone alveolar count (RAC) and lung weight/body weight ratio (LW/BW), which respectively represent the average alveolar diameter, alveolar separation and alveolar generation, and the increase of cells and pulmonary edema.

*Cell culture and construction of BPD model in vitro*

Human lung epithelial cell line BEAS-2B (Chuanqiu Biotechnology Co., Ltd., Shanghai, China, HM084) was purchased and cultured in RPMI-1640 medium (Guduo Biotechnology Co., Ltd., Shanghai, China, GD-A509) at 37°C with 5% $CO_2$, which contained 10% fetal bovine serum (FBS) (Lianshuo Biotechnology Co., Ltd., Shanghai, China, China) and 1% penicillin/streptomycin (Guduo Biotechnology Co., Ltd., Shanghai, China, GD-Y1033). The cells were inoculated in a 6-well plate for incubation for 24 hours, and then placed in RPMI-1640 medium (containing 0.1% FBS) for 6 h. Then, cells incubated in indoor air for 6 hours were used as Con group, and cells incubated in high oxygen environment for 6 hours were used as Hyperoxia group [19].

*Cell transfection*

Cell transfection was carried out by Lipofectamine 2000 transfection reagent (Hengfei Biotechnology Co., Ltd., Shanghai, China, 11 668019). Con+si-MALAT1 group, Con+si-NC group, Hyperoxia+si-MALAT1 group and Hyperoxia+si-NC group were transfected with si-MALAT1 and si-NC on the basis of Con group and Hyperoxia group. In addition, in the co-transfection experiment, the Hyperoxia+si-MALAT1 group was additionally transfected with inhibitor-NC or inhibitor.

*RT-PCR*

Total RNA of serum, lung tissue and BEAS-2B cells was extracted by TRIzol reagent (Yuduo Biotechnology Co., Ltd., Shanghai, China, YDJ-2531), and then reverse transcribed by reverse transcription kit (Xinyu Biotechnology Co., Ltd., Shanghai, China, 60906-10). qPCR was carried out for cDNA by SYBR Premix Ex TaqTM II kit (Yihui Biotechnology Co., Ltd., Shanghai, China, HRR041A-1). GAPDH was applied as internal reference for MALAT1, and U6 for miR-206. The relative gene expression was calculated by $2^{-\Delta\Delta CT}$.

*Enzyme linked immunosorbent assay (ELISA)*

The inflammatory indicators TNF-α, IL-1β and MCP-1 were detected by ELISA kits (Lvyuan Bode Biotechnology Co., Ltd., Beijing, China, mouse TNF-α, mouse IL-1β and mouse MCP-1), and the operation steps were strictly in accordance with the instructions.

*Determination of oxidative stress*

Referring corresponding detection kits (Zhen Shanghai and Shanghai Industrial Co., Ltd., Shanghai, China, HZ-MDA-Ge, HZ-SOD-Ra), the activities of malondialdehyde (MDA) and superoxide dismutase (SOD) were detected, and the operation steps were strictly in accordance with the instructions.

*TUNEL*

The apoptosis of mouse left lung tissue was detected by TUNEL kit (Shanghai C-reagent Biotechnology Co. Ltd., Shanghai, China, CSX-9724). A 50 μL TUNEL reaction solution was added to mouse tissue slices, 50 μL peroxidase was added after 50 min, incubated at 37°C for 30 min, dyed with 100 μL diaminobenzidine (DAB) working solution for 10 min, re-dyed with hematoxylin for 3 s, and sealed with neutral resin. Finally, 5 regions randomly selected from each group were observed by high power microscope and the apoptosis rate was calculated.

*Determination of apoptosis*

The apoptosis was determined by annexin V-fluorescein isothiocyanate (FITC)/propidium iodide (PI) apoptosis detection kit (Xinfan Biotechnology Co., Ltd., Shanghai, China, XB2210-100T). Cells were collected with 0.25% trypsin (Yuanye Biotechnology Co., Ltd., Shanghai, China, R20109), washed with phosphate buffer (PBS) (Hengfei Biotechnology Co., Ltd.,

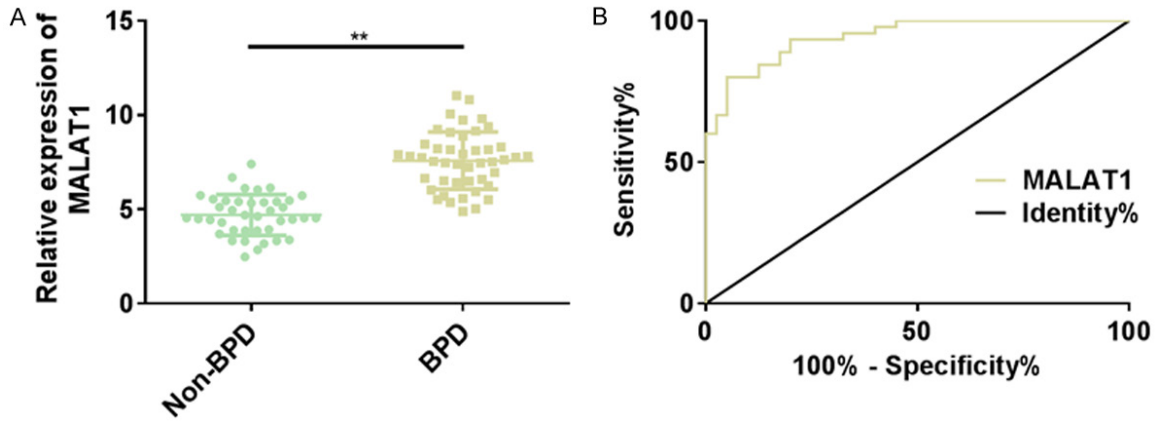


**Figure 1.** Expression of serum MALAT1 in neonatal BPD. We detected the serum MALAT1 of neonatal BPD and normal newborns in the same period by RT-PCR, and found that the serum MALAT1 of neonatal BPD was evidently enhanced (A). We also visualized ROC curve for distinguishing neonatal BPD and normal newborns in the same period, with an area under the curve as high as 0.943 (B). Note: ** indicates compared between two groups, P<0.01.

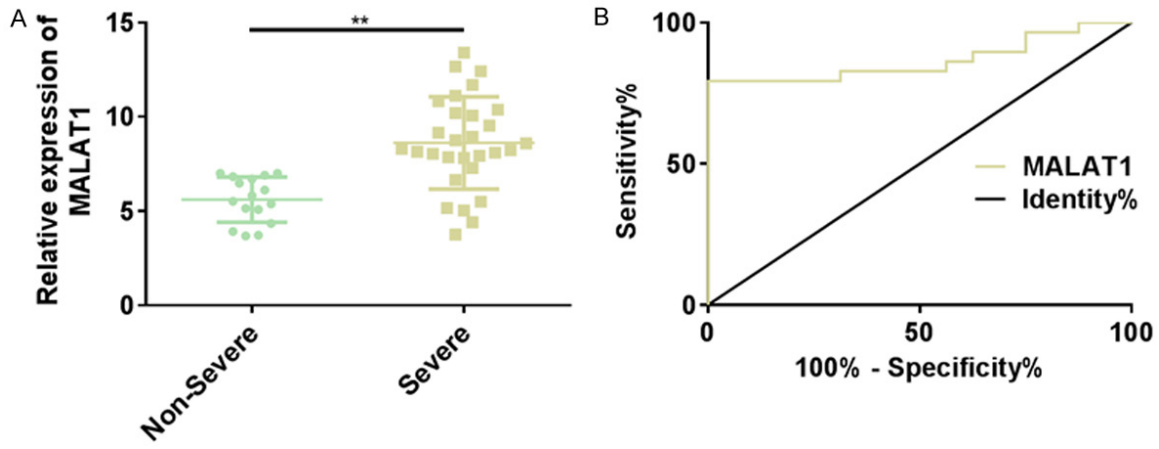


**Figure 2.** MALAT1 in severe BPD of newborn and its predictive value. MALAT1 in neonatal BPD serum was detected by RT-PCR. By further grouping the severity of BPD, we found that (A) the expression of MALAT1 in Non-Severe group was evidently lower than that in Severe group. (B) The area under the curve for MALAT1 to distinguish severe BPD was 0.866. Note: ** indicates compared with Non-Severe, P<0.01.

Shanghai, China, R22119), and then stained with 5 μL Annexin V-FITC and 5 μL PI for 30 min in the dark at room temperature. Apoptosis was analyzed by flow cytometry (Beijing Image Trading Co., Ltd., Beijing, China, AMG-0002051).

*Detection of double luciferase reporter gene*

Wild-type and mutant target fragments of MALAT1 were constructed and corresponding vectors (MALAT1-Wt, MALAT1-Mut) were established by loading pGL3. miR-129-5p and miR-NC were co-transfected into BEAS-2B cells. After transfection for 48 h, luciferase activity was determined according to the operating instructions of the dual luciferase reporter molecular assay system (Zeye Biotechnology Co., Ltd., Shanghai, China, 11402ZY60).

*RNA immunoprecipitation (RIP) experiment*

Magna RIP kit (Yihui Biological Technology Co., Ltd., Shanghai, China, MAGNARIP01-1) was applied for RIP analysis, and the experimental process was strictly in accordance with the instructions. The cells were lysed, incubated with protein A magnetic beads, and conjugated with antibodies (4°C). After 6 hours, the beads were washed and incubated with 0.1% SDS and 0.5 mg/ml proteinase K at 55°C for 30 min. Finally, RT-qPCR was performed for the purified RNA with gene-specific primers to verify the target.

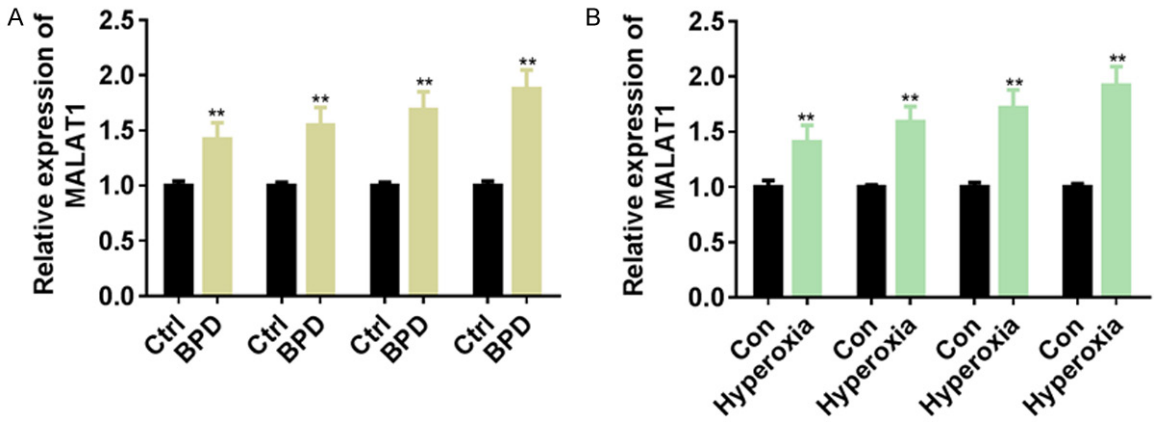


**Figure 3.** MALAT1 expression in BPD model. RT-PCR was used to detect the expression of MALAT1 in BPD in vivo model (A) or in vitro model (B) at different induction time, and MALAT1 was abnormally up-regulated in BPD model. Note: ** indicates compared with Ctrl or Con, P<0.01; a indicates compared with 0 d, P<0.05.

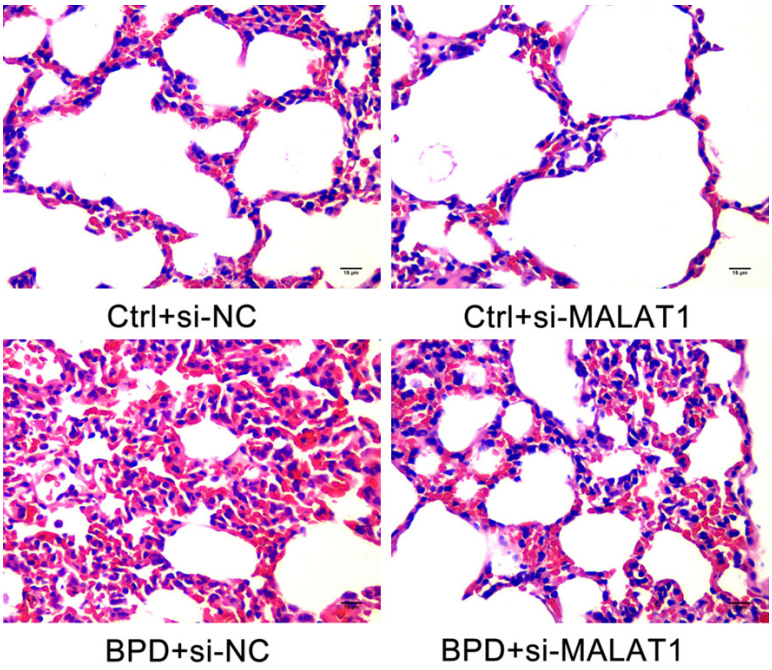


**Figure 4.** HE staining was used to evaluate the effect of MALAT1 on lung tissue of BPD model in vivo. Scale: 15 μm; Magnification: 400.

*Pathological assessment*

We mainly assessed the morphology of the left lung of mice by HE dying. The positive expression rate of Ki67 or platelet endothelial cell adhesion molecule-1 (CD31) protein was detected by immunohistochemistry.

*Statistical analysis*

The experiments were carried out independently and repeatedly for three times. The data were analyzed by SPSS 17.0 and represented by mean ± standard deviation. The differences of the data were analyzed by student t-test or 2-way ANOVA, and evaluated by receiver operating characteristic curve (ROC). P<0.05 was considered to have statistical differences.

## Result

*Serum MALAT1 was up-regulated in neonatal BPD*

To understand whether MALAT1 as a serum index can indicate the abnormality of BPD, we compared the serum MALAT1 between neonatal BPD and normal newborns at the same time. The results showed that serum MALAT1 was highly expressed in neonatal BPD (**Figure 1A**), and the area under the curve for identifying neonatal BPD was 0.943 (**Figure 1B**), with sensitivity and specificity of 80.00% and 95.00%, respectively, suggesting that MALAT1 had great potential as a biomarker of BPD. See **Figure 1**.

*Serum MALAT1 was associated with severe BPD in neonates*

We also explored whether MALAT1 responded to BPD. The data showed that MALAT1 was evi-

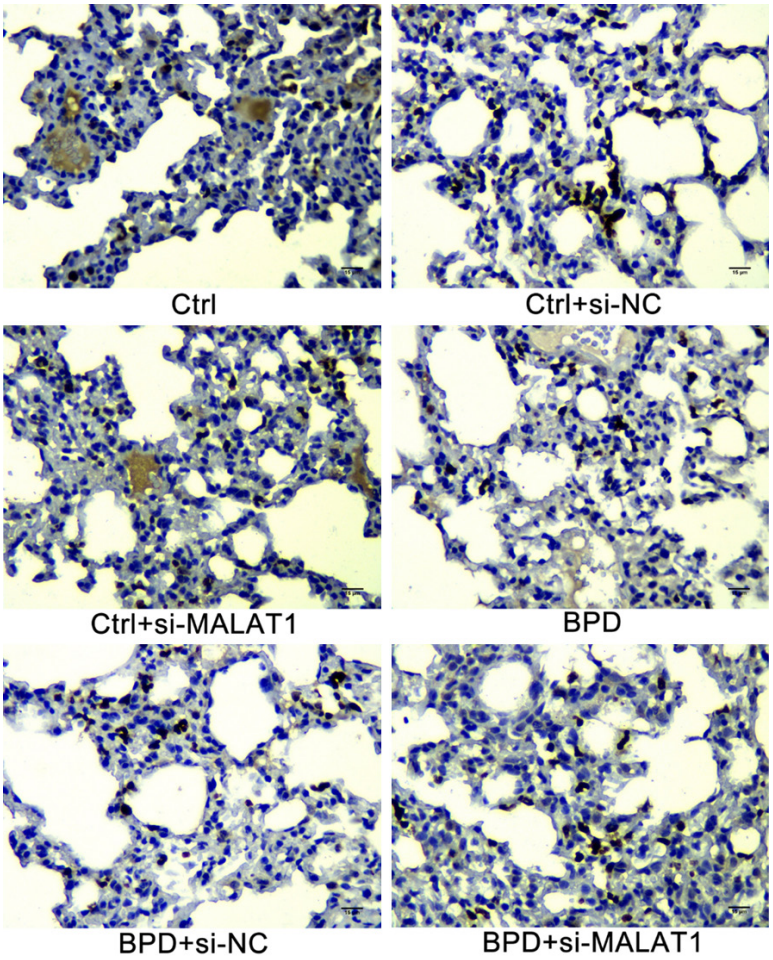


**Figure 5.** Immunohistochemical analysis of MALAT1 on the positive expression rate of Ki67 protein in BPD model in vivo. Scale: 15 μm; Magnification: 400.

dently higher in severe BPD than in non-severe BPD (**Figure 2A**), suggesting that MALAT1 may be helpful to indicate the condition of BPD. In addition, we also found that the area under the curve was 0.866 (**Figure 2B**), and the sensitivity and specificity were 79.31% and 100.00%, respectively, indicating that it may also have better value in distinguishing severe BPD. See **Figure 2**.

*MALAT1 was also up-regulated in BPD in vivo and in vitro*

We also verified the expression of MALAT1 in BPD model. The results showed that MALAT1 was evidently up-regulated in BPD models both in vivo (**Figure 3A**) and in vitro (**Figure 3B**), and this up-regulation was strengthened with the induction time of the model. This suggested that it may be highly responsive to the occurrence and progression of MALAT1. See **Figure 3**.

*Pathological effects of MALAT1-miR-206 axis on BPD model in vivo*

In order to explore the role of MALAT1-miR-206 axis, we evaluated the lung tissue of BPD model in vivo. HE dying analysis showed that compared with Ctrl+si-NC or Ctrl+si-MALAT1 group, the number of alveoli in BPD+si-NC group increased evidently, and the alveolar space and fusion decreased evidently, while those in BPD+si-MALAT1 group improved evidently (**Figure 4**). Immunohistochemical analysis showed that the positive expression rate of Ki67 (**Figure 5**) or CD31 protein (**Figure 6**) in BPD+si-NC group was evidently lower than that in Ctrl+si-NC or Ctrl+si-MALAT1 group, while the above indexes were evidently up-regulated in BPD+si-MALAT1 group (**Figure 10A**, **10B**). The above results were the same in miR-206, that is, BPD+miR-206 group could alleviate the pathological results of alveoli (**Figure 7**) and the positive expression rate of Ki67 (**Figure 8**) or CD31 (**Figure 9**) protein in different degrees (**Figure 10C**, **10D**). All the above results indicated that knocking down MALAT1 or up-regulating miR-206 could treat or improve the disease progression of BPD in different degrees. See **Figures 4**-**10**.

*Knocking down MALAT1 had protective effect on BPD in vivo model*

In order to further understand the specific mechanism of MALAT1 in BPD, we explored in vivo and in vitro. At first, we realized the construction of MALAT1 knock-down model by injecting si-MALAT1 into BPD in vivo model (**Figure 11A**). Then, we measured MLI, RAC and LW/BW to evaluate the degree of alveolization and lung injury in each group of mice. Compared with Ctrl group, MLI (**Figure 11B**) and LW/BW

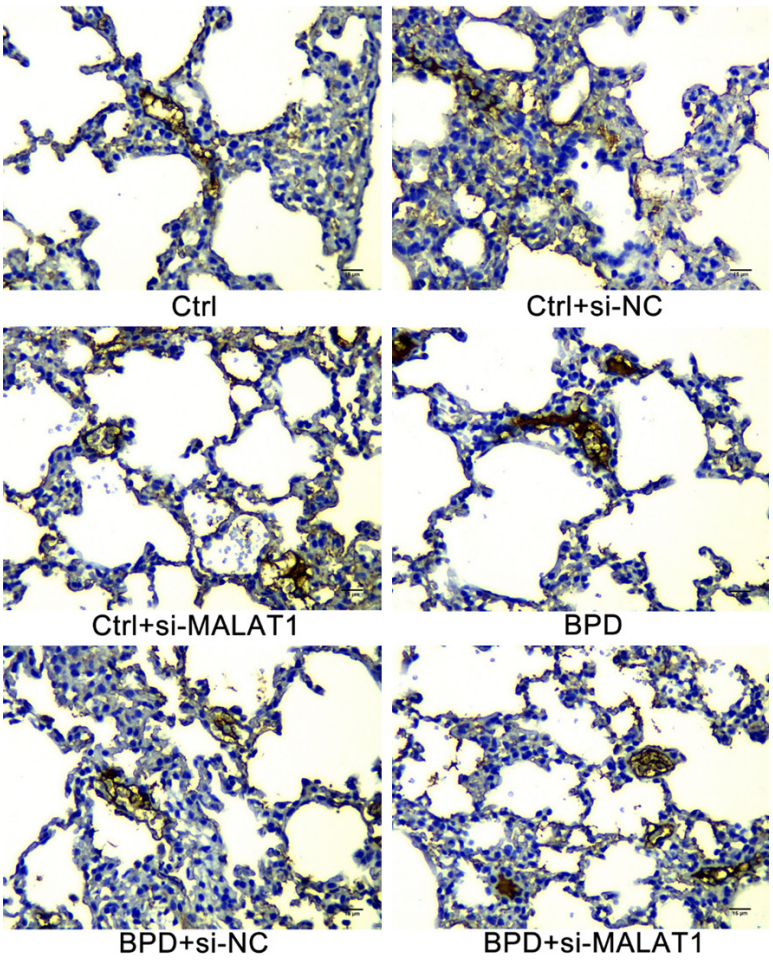


**Figure 6.** Immunohistochemical analysis of MALAT1 on the positive expression rate of CD31 protein in BPD model in vivo. Scale: 15 μm; Magnification: 400.

(**Figure 11C**) in BPD group increased evidently, while RAC (**Figure 11D**) decreased evidently, and BPD+si-NC group had similar results. In addition, Ctrl+si-NC group and Ctrl+si-MALAT1 group had similar results with Ctrl group. In BPD+si-MALAT1 group, the above indexes were evidently reversed, that is, MLI and LW/BW decreased and RAC increased. On the other hand, we also explored the effects of knocking down MALAT1 on inflammation, oxidative stress and apoptosis of BPD model in vivo. Compared with Ctrl group, TNF-α (**Figure 11E**), IL-1β (**Figure 11F**) and MCP-1 (**Figure 11G**) in BPD group were evidently higher, MDA (**Figure 11H**) was evidently higher, SOD (**Figure 11I**) was evidently lower, and apoptosis level was evidently improved (**Figures 11J**, **12**). However, under the influence of si-MALAT1, the above indexes were evidently improved. All the above results suggested that knocking down MALAT1 was helpful to improve alveolarization, lung injury, inflammation, oxidative stress and apoptosis of BPD model in vivo. See **Figures 11** and **12**.

*Knocking down MALAT1 haD protective effect on BPD model in vitro*

We explored the effect of knocking down MALAT1 on BPD model in vitro. Firstly, we realized the down-regulation of MALAT1 by transfecting si-MALAT1 (**Figure 13A**). Compared with Con group, TNF-α (**Figure 13B**), IL-1β (**Figure 13C**), IL-1β (**Figure 13D**) and other inflammatory cytokines in Hyperoxia group increased evidently, MDA (**Figure 13E**) increased evidently, SOD (**Figure 13F**) decreased evidently and apoptosis level increased evidently (**Figure 13G**). However, all the above indexes in Hyperoxia+si-MALAT1 group improved to varying degrees. In addition, the results of Con+si-NC group and Con+si-MALAT1 group were similar to Con group, and the results of Hyperoxia+si-NC group and Hyperoxia group were similar. All the results showed that knocking down MALAT1 also had a certain degree of protection in vitro for BPD model in vitro, which is mainly reflected in relieving inflammation, oxidative stress and apoptosis. See **Figure 13**.

*MALAT1 had a targeted relationship with miR-206*

In order to further explore the protective mechanism of knocking down MALAT1 on BPD model, we carried out relevant biological analysis. There were potential conservative binding sites between them through StarBase (**Figure 14A**). In the results of double luciferase gene report, miR-206 had a significant inhibitory effect on MALAT1-Wt, but had no significant effect on MALAT1-Mut (**Figure 14B**). In RIP analysis, Ago2 had great recruitment ability for both (**Figure 14C**). In addition, the expression

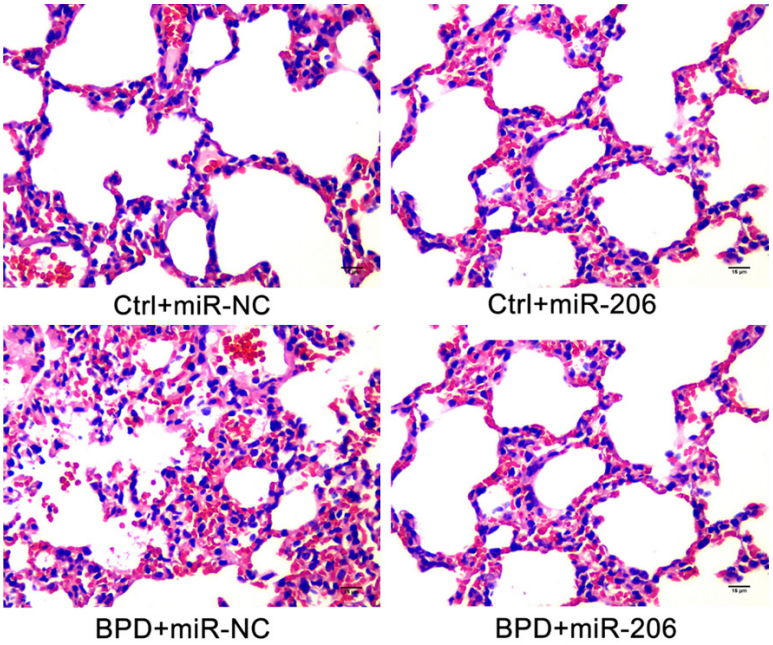


**Figure 7.** HE staining was used to evaluate the effect of miR-206 on lung tissue of BPD model in vivo. Scale: 15 μm; Magnification: 400.

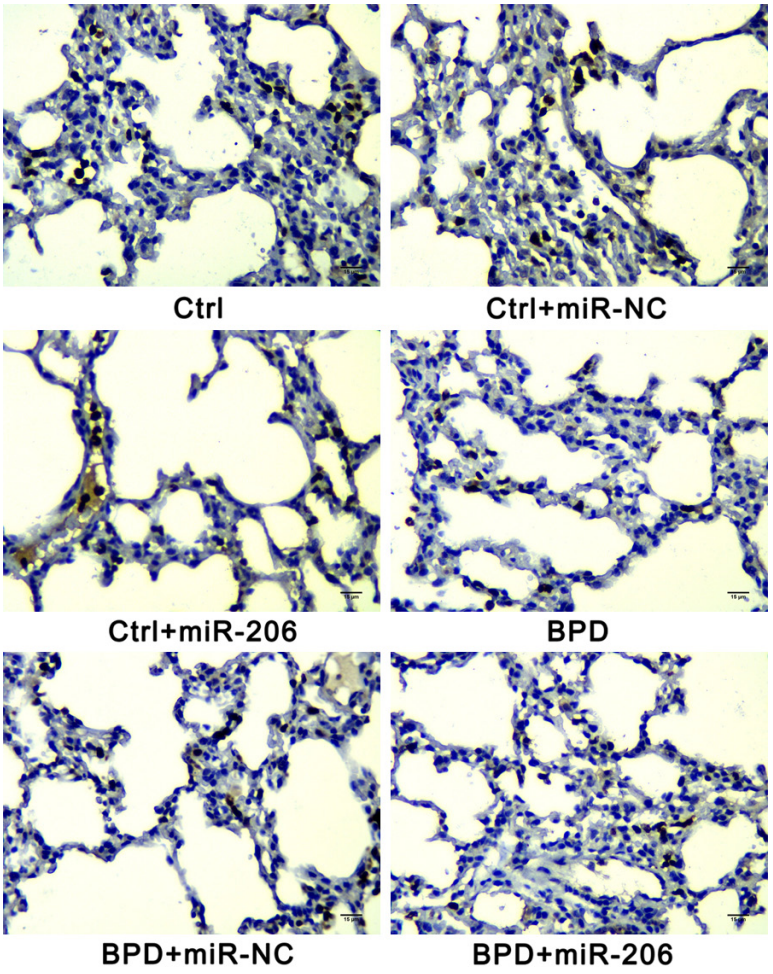


**Figure 8.** Immunohistochemical analysis of the effect of miR-206 on the positive expression rate of Ki67 protein in BPD model in vivo. Scale: 15 μm; Magnification: 400.

of miR-206 was negatively regulated by MALAT1, and the expression of miR-206 was obviously up-regulated in cells transfected with si-MALAT1 (**Figure 14D**). miR-206 was detected to be evidently down-regulated in BPD in vivo and in vitro (**Figure 14E**). The above results suggested that, firstly, miR-206 had a targeted relationship with MALAT1. Second, miR-206 may be related to the occurrence and development of BPD. See **Figure 14**.

*Down-regulation of miR-206 could counteract the anti-BPD effect of knocking down MALAT1*

In order to understand the specific molecular mechanism of MALAT1-miR-206 axis in BPD, we also conducted similar in vitro studies. At first, we down-regulated the expression of miR-206 by transfecting inhibitor, and we found that the expression of miR-206 after co-transfection of inhibitor+si-MALAT1 was almost the same as that of inhibitor-NC group (**Figure 15A**), which indicated that the expression of miR-206 was regulated by MALAT1 and confirmed the targeted regulation relationship between them. Then, we also explored from inflammation, oxidative stress and apoptosis. Compared with Hyperoxia+si-MALAT1 group or Hyperoxia+si-MALAT1+ inhibitor-NC group, the improvement of inflammation (**Figure 15B-D**), oxidative stress

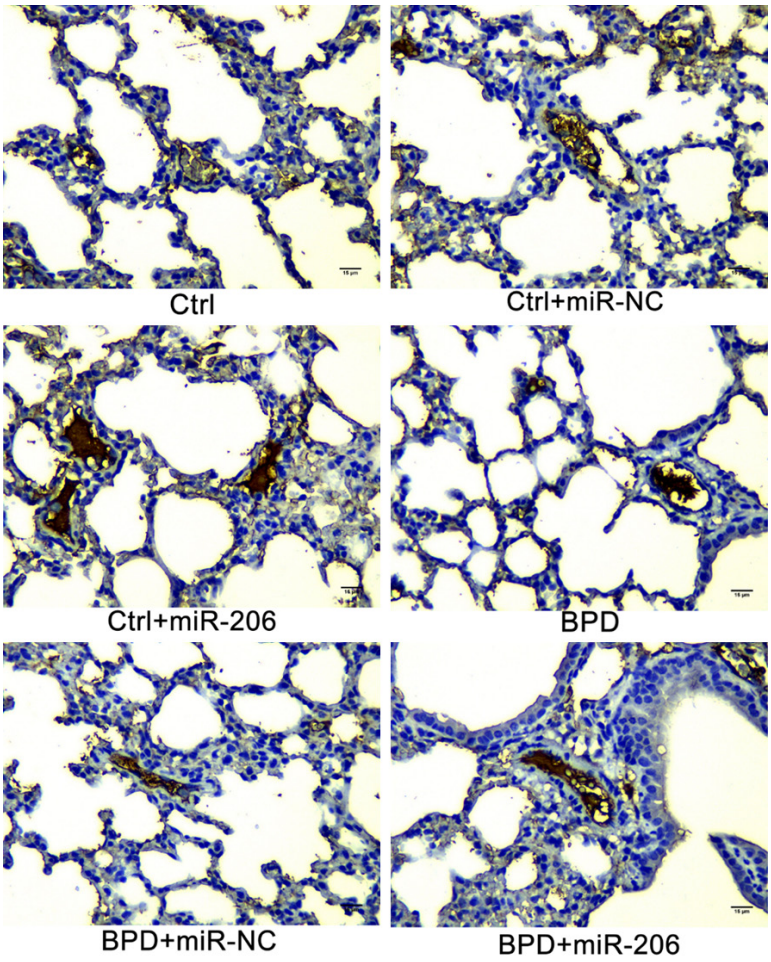


**Figure 9.** Immunohistochemical analysis of miR-206 on the positive expression rate of CD31 protein in BPD model in vivo. Scale: 15 μm; Magnification: 400.

(**Figure 15E**, **15F**) and apoptosis (**Figure 15G**) in Hyperoxia+si-MALAT1+inhibitor group was eliminated to varying degrees, and the above three indexes all developed towards Hyperoxia+si-NC group. The above results indicated that down-regulation of miR-206 could also eliminate the anti-BPD effect in vitro after knocking down MALAT1. In conclusion, knocking down MALAT1 has different therapeutic effects on BPD model, such as anti-inflammatory, anti-oxidative stress and anti-apoptosis, and this protective mechanism is mediated by miR-206, that is, MALAT1-miR-206 axis may become a new therapeutic target for BPD. See **Figure 15**.

## Discussion

Pulmonary hypoplasia caused by BPD may cause respiratory insufficiency, which is the main cause of perinatal morbidity and mortality of newborns [20]. At present, BPD has become a difficult problem in the treatment of newborn premature infants, and the research on molecular level is not yet clarified. Therefore, it is of great value to explore the biomarkers and molecular mechanism of BPD for improving the outcome of BPD.

LncRNA participates in the pathogenesis of many human diseases by mediating various molecular mechanisms, and also has a certain regulatory effect on the physiological and pathological process of the lung. For example, in chronic obstructive pulmonary disease, maternal expression gene 3 (MEG3) is evidently over-expressed, and the apoptosis of human pulmonary microvascular endothelial cells is further promoted by up-regulating the expression of pro-apoptotic protein [21]. In addition, MALAT1 could promote epithelial-mesenchymal transition (EMT) induced by respiratory particles by regulating miR-204-ZEB1 axis [22]. In this study, we found that MALAT1, as a serum marker, was evidently up-regulated in neonatal BPD, and in severe BPD, relatively non-severe BPD was also up-regulated, indicating that MALAT1 may have a certain response to this disease. It is known that MALAT1 exists in various tissues of human body to varying degrees, and is most active in lung [23]. Although it can protect premature infants with BPD to a certain extent, it will further activate inflammatory micro-environment and worsen BPD by up-regulating high mobility group box 1 protein (HMGB1) during the development of BPD [10]. Furthermore, the area under the curve of MALAT1 for differentiating neonatal BPD from severe BPD was 0.943 and 0.866, respectively, suggesting that MALAT1 may be used as a biomarker for screening BPD and predicting severe BPD. It is reported that MALAT1 is also evidently up-regulated in non-

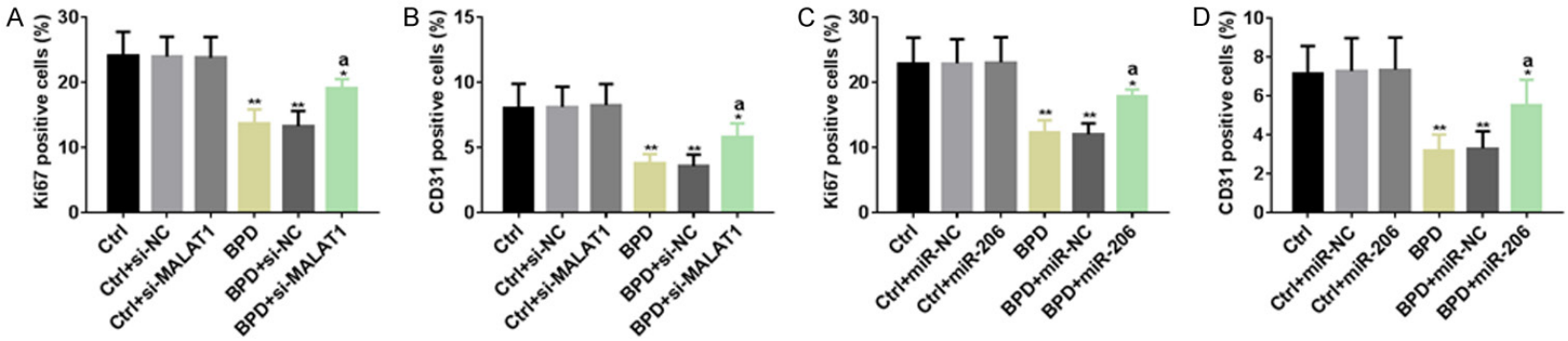


**Figure 10.** Statistical analysis results of Ki67 and CD31 protein positive expression rate in BPD in vivo model. The effects of MALAT1 and miR-206 on the positive expression rate of (A, C) Ki67 and (B, D) CD31 protein in BPD models were detected by immunohistochemistry. Note: * indicates compared with Con or Ctrl, $P<0.05$; ** indicates $P<0.01$; a indicates compared with BPD or Hyperoxia, $P<0.05$.

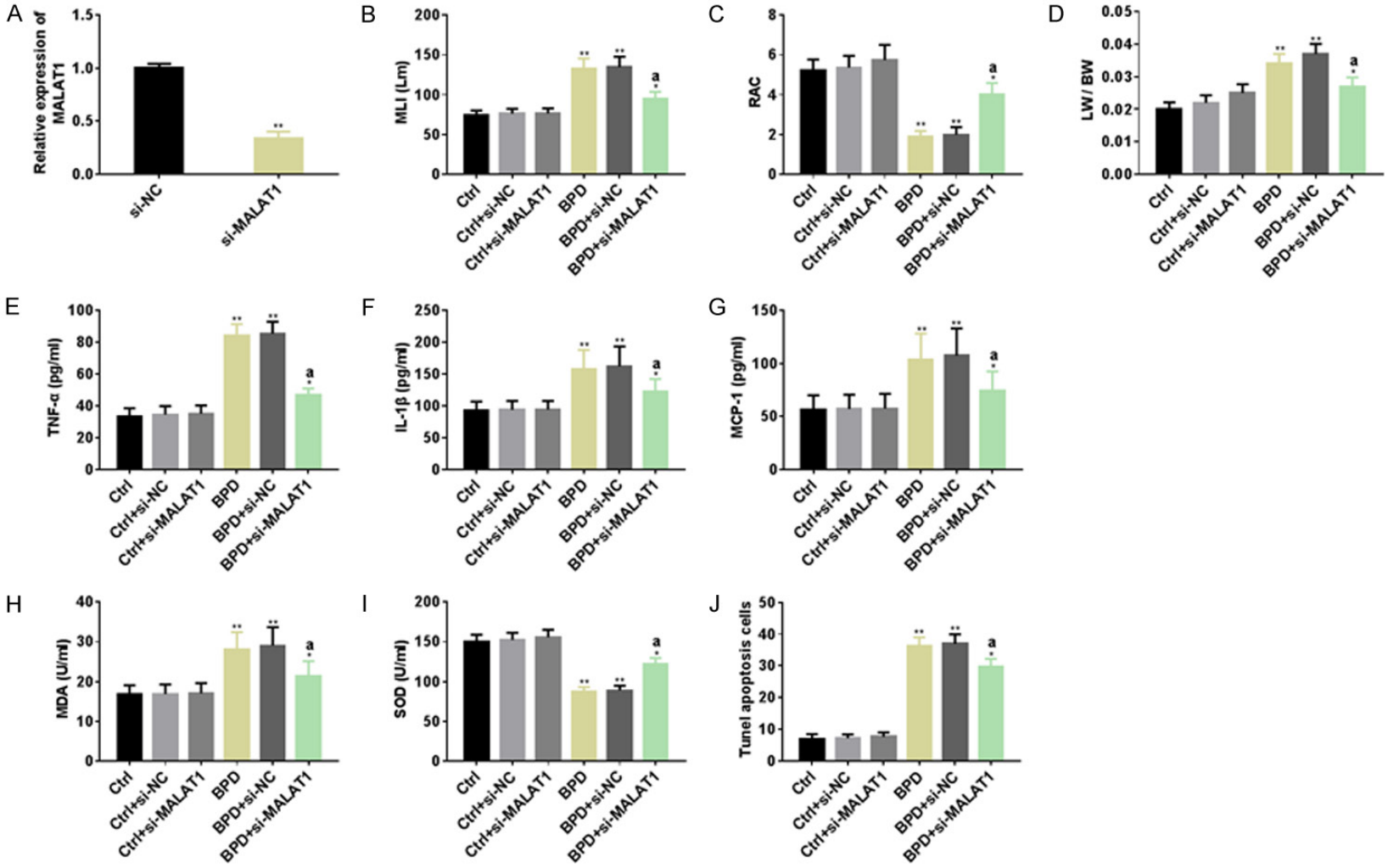


**Figure 11.** Effect of knocking down MALAT1 on BPD in vivo model. At first, we tested the transfection efficiency of MALAT1 by RT-PCR (A), and successfully realized the knock-down model of MALAT1 by transfecting si-MALAT1 to BPD in vivo model. Then, seven days after the intervention of si-MALAT1, we measured (B) MLI, (C) RAC and (D) LW/BW of each group, and measured the inflammatory indexes such as (E) TNF-α, (F) IL-1β and (G) MCP-1 in serum of each group by ELISA. (H) MDA, (I) SOD and other oxidative stress indexes were detected by the corresponding detection kit, and the apoptosis level was measured by (J) TUNEL. Note: * indicates compared with Ctrl, $P<0.05$; ** indicates $P<0.01$; a indicates compared with BPD, $P<0.05$.

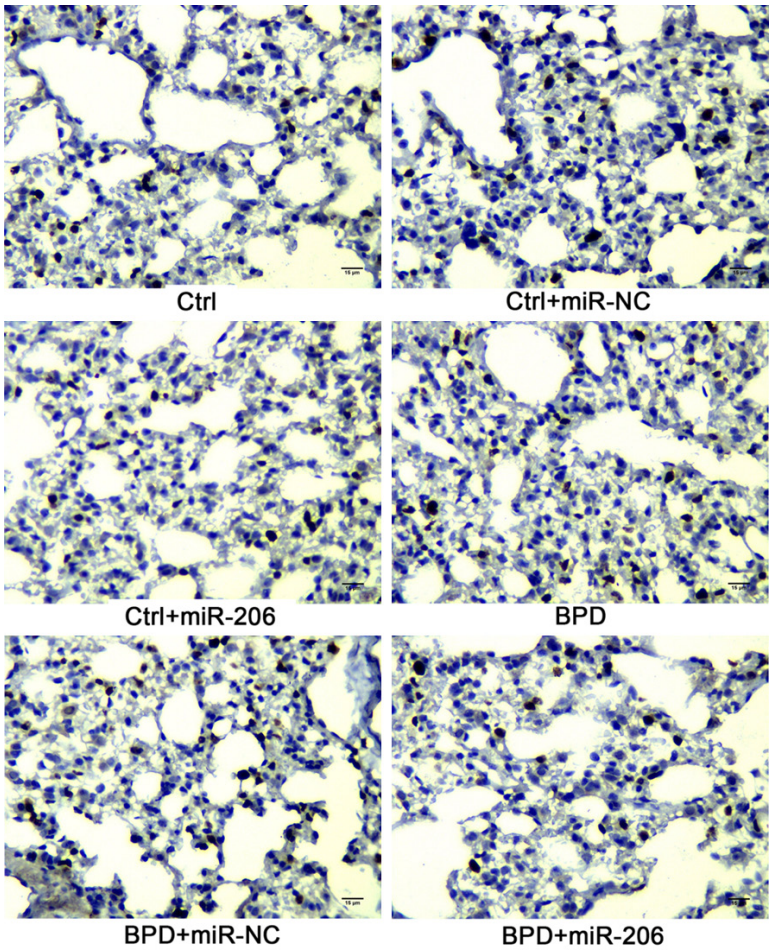


**Figure 12.** TUNEL method was used to explore the effect of knocking down MALAT1 on apoptosis level of BPD model cells in vivo. Scale: 15 μm; Magnification: 400.

small cell lung cancer (NSCLC), and can be used as a prognostic biomarker to predict the survival of patients [24]. In cell experiment, we established BPD models in vivo and in vitro with C57BL/6J mice and BEAS-2B cells and found that MALAT1 was up-regulated in BPD models in vivo and in vitro, and the expression increased with the induction time of the model. Our research data showed that up-regulation of miR-206 or down-regulation of MALAT1 improved the pathological condition of BPD in vivo model, which is mainly reflected in the improvement of alveolar pathological condition and the up-regulation of Ki67 and CD31 protein positive expression rate. Ki67 is a nuclear antigen, which is related to cell proliferation, and is beneficial to reflect the replication ability of cells [25]. However, CD31 is a marker of endothelial cells, and its expression level will be inhibited when exposed to high oxygen, which will strengthen the process of endothelial-mesenchymal transition and is not conducive to the reversal of BPD [26]. On the other hand, obvious inflammatory reaction, oxidative stress and evidently up-regulated apoptosis were observed in BPD models in vivo and in vitro. In addition, we also found in BPD mice that MLI and LW/BW increased, while RAC decreased evidently. However, after MALAT1 knockdown treatment, the above abnormal phenomena were alleviated to varying degrees. We also found the regulatory mechanism of MALAT1 in BPD in different reports. In the research of Cai et al. [2], MALAT1 was highly expressed in the lung tissue of BPD mice and the blood of premature infants, and its up-regulation could play a protective role by inhibiting apoptosis. Yangi et al. [10] pointed out that there is a process of controlling BPD by MALAT1-miR-129-5p-high mobility group protein 1 (HMGB1) molecular network, and up-regulation of MALAT1 can evidently promote the vitality and inflammatory response of BEAS-2B cells. The above reports were different from our research results, but there is no doubt that MALAT1 has certain molecular influence on BPD process.

miRNA is a short-chain RNA molecule, which can regulate gene expression like LncRNA, and then affect the physiological and pathological process of the body [27]. It is known that miRNA can be regulated by LncRNA sponge and participate in the pathological process of various lung diseases. For example, knocking down XIST can inhibit the survival and metastasis of NSCLC cells by up-regulating miR-144-3p [28]. PVT1 regulates asthma induced by respiratory syncytial virus by targeting miR-203a, and mediates α asarone-mediated protective mechanism [29]. In our study, MALAT1 had a targeted

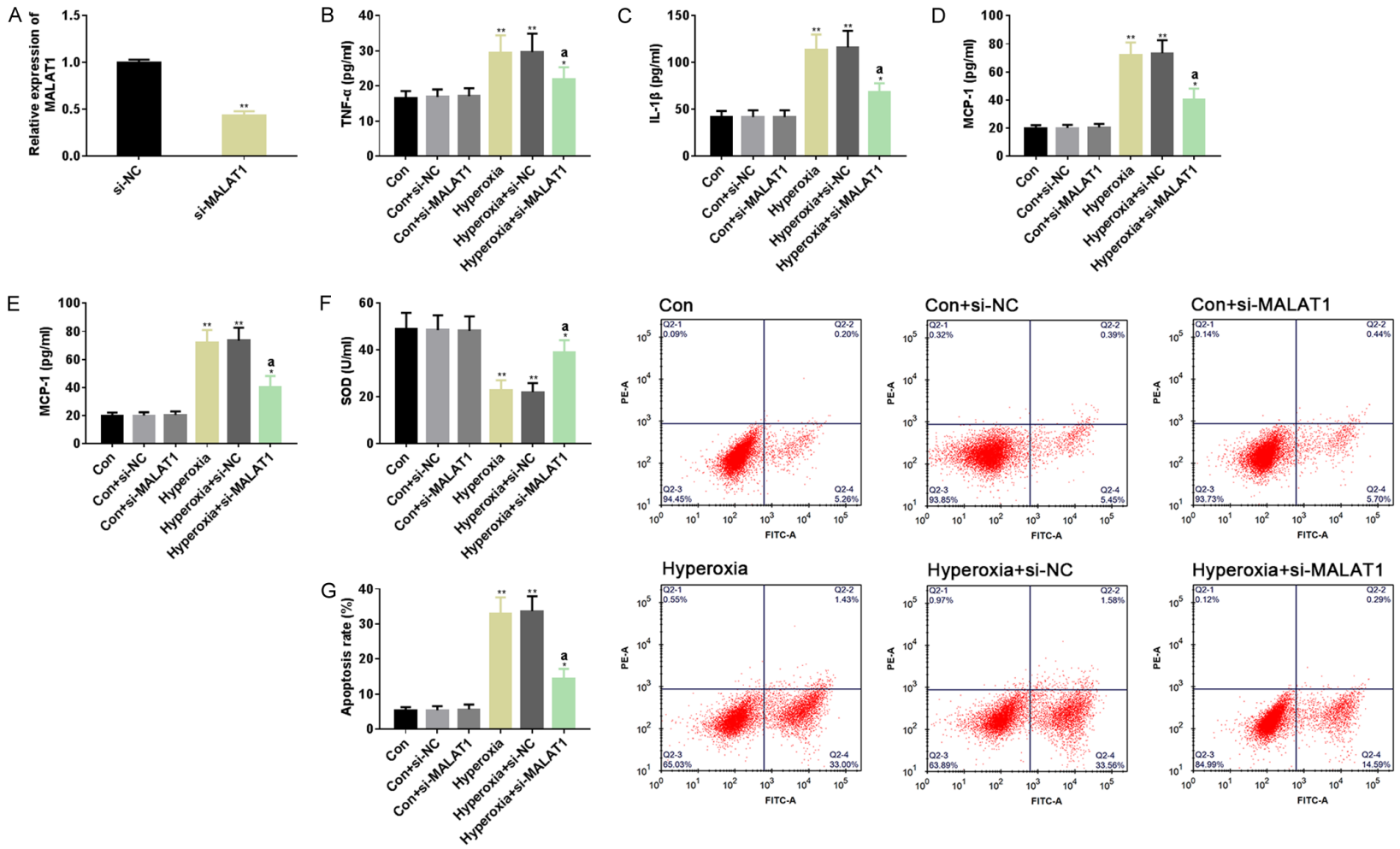


**Figure 13.** Effect of knocking down MALAT1 on BPD model in vitro. We also tested the transfection efficiency of MALAT1 in BPD in vitro model by RT-PCR (A), and successfully down-regulated MALAT1 in BPD in vitro model by transfection of si-MALAT1. Then, we measured the inflammatory indexes such as (B) TNF-α, (C) IL-1β and (D) MCP-1 in serum of each group by ELISA, detected the oxidative stress indexes such as (E) MDA and (F) SOD by corresponding detection kits, and tested the apoptosis level by flow cytometry (G). Note: * indicates compared with si-NC/Con, P<0.05; ** indicates P<0.01; a indicates compared with Hyperoxia, P<0.05.

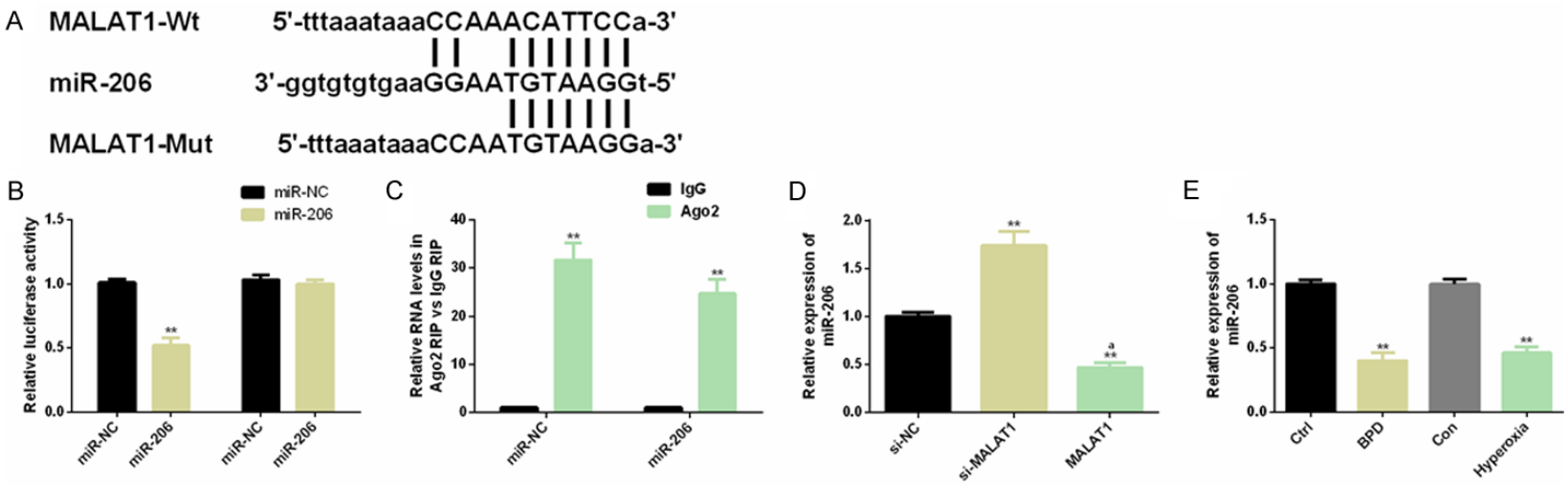


**Figure 14.** Relationship between MALAT1 and miR-206. The relationship between miR-206 and MALAT1 was confirmed by (A) StarBase, and further verified by (B) double luciferase report and (C) RIP analysis. In addition, we also detected the expression of miR-206 under the influence of (D) MALAT1 and in (E) BPD model in vitro and in vivo by RT-PCR. Note: ** indicates compared with miR-NC/si-NC/IgG/Ctrl/Con, $P<0.01$; a indicates compared with si-MALAT1, $P<0.05$.

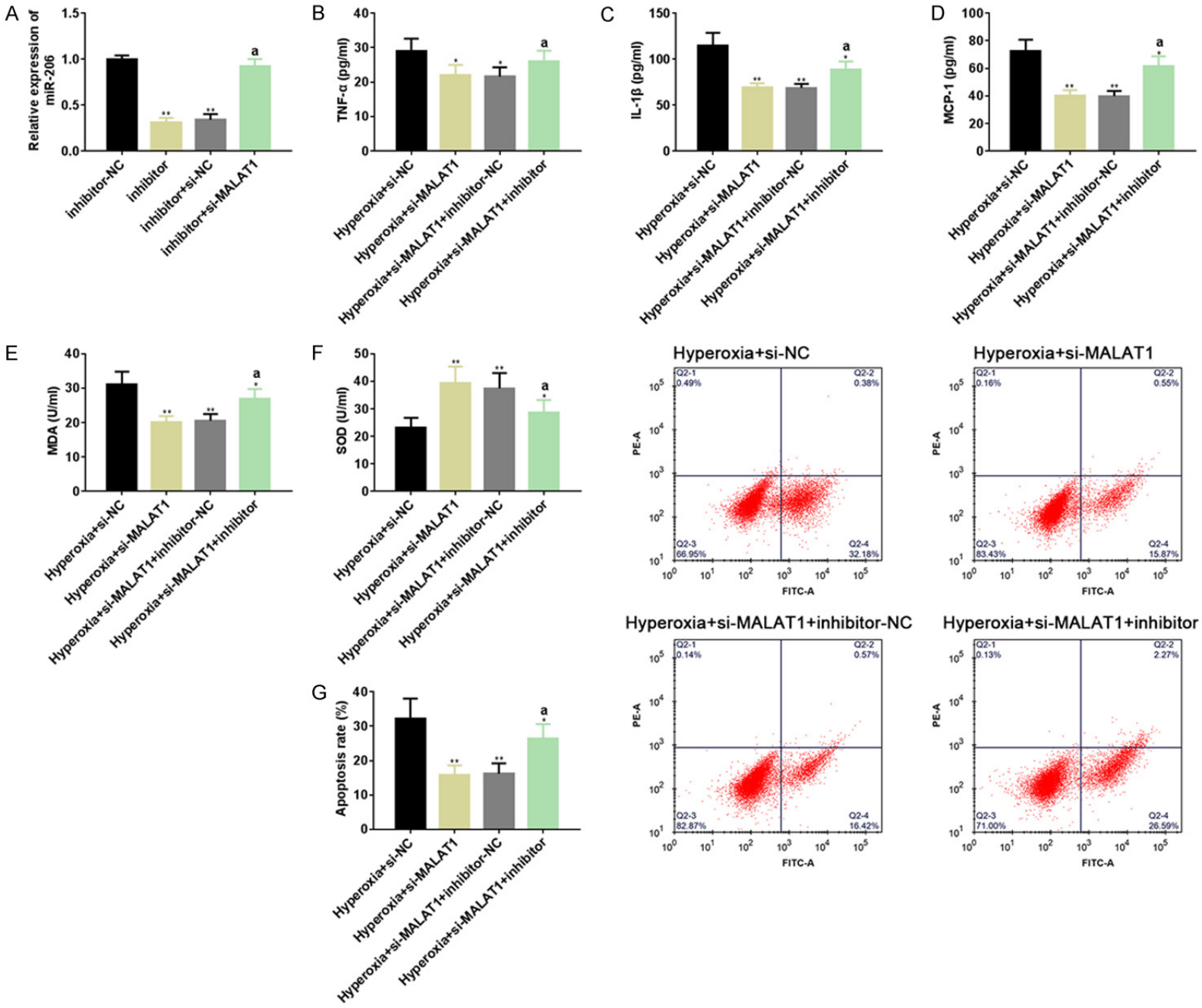
A
Relative expression of miR-206
inhibitor-NC
inhibitor
inhibitor+si-NC
inhibitor+si-MALAT1
B
TNF-α (pg/ml)
C
IL-1β (pg/ml)
D
MCP-1 (pg/ml)
Hyperoxia+si-NC
Hyperoxia+si-MALAT1
Hyperoxia+si-MALAT1+inhibitor-NC
Hyperoxia+si-MALAT1+inhibitor
E
MDA (U/ml)
F
SOD (U/ml)
G
Apoptosis rate (%)
Hyperoxia+si-NC
Q2-1 0.49%
Q2-2 0.38%
Q2-3 66.95%
Q2-4 32.18%
Hyperoxia+si-MALAT1
Q2-1 0.16%
Q2-2 0.55%
Q2-3 83.43%
Q2-4 15.87%
Hyperoxia+si-MALAT1+inhibitor-NC
Q2-1 0.14%
Q2-2 0.57%
Q2-3 82.87%
Q2-4 16.42%
Hyperoxia+si-MALAT1+inhibitor
Q2-1 0.13%
Q2-2 2.27%
Q2-3 71.00%
Q2-4 26.59%
PE-A
FITC-A

**Figure 15.** Effect of down-regulating miR-206 on the anti-BPD effect of knocking down MALAT1. We detected the transfection efficiency of miR-206 and MALAT1 in BPD in vitro model by RT-PCR (A), and successfully down-regulated miR-206 in BPD in vitro model by transfection of inhibitor. Then, we measured the inflammatory indexes such as (B) TNF-α, (C) IL-1β and (D) MCP-1 in serum of each group by ELISA, detected the oxidative stress indexes such as (E) MDA and (F) SOD by corresponding detection kits, and tested the apoptosis level by flow cytometry (G). Note: * indicates compared with inhibitor-NC/Con, $P<0.05$; ** indicates $P<0.01$; a indicates compared with inhibitor, $P<0.05$.

relationship with miR-206, and miR-206 was down-regulated in BPD in vivo and in vitro. Previous studies have shown that miR-206 plays a regulatory role in BPD models in vivo and in vitro, and can target fibronectin 1 (FN1) to influence the progress of BPD [30]. FN1 is a glycoprotein that can regulate the remodeling of extracellular matrix (ECM), and the abnormal remodeling of ECM is involved in the pathogenesis of BPD [15]. Based on the above research, the results of up-regulating miR-206 or knocking down MALAT1 suggested that this may have a certain therapeutic effect on neonatal BPD, and developing corresponding biological agents may be a good treatment choice. In addition, we also conducted a co-transfection study at last. In short, down-regulation of miR-206 can also eliminate the anti-BPD effect of knocking down MALAT1, which threatens the anti-inflammatory, anti-oxidative stress and anti-apoptosis effect of knocking down MALAT1 to varying degrees. This further indicated that MALAT1-miR-206 axis can regulate the development of BPD and can be used as a new therapeutic target.

Although our research has confirmed that MALAT1 can not only be used as a biomarker of neonatal BPD, knocking down its expression is also beneficial to inhibit the course of BPD. However, there is still room for improvement in our research. First of all, we can supplement the downstream molecular mechanism of miR-206 and further supplement the relevant regulatory factors. Secondly, we can increase the analysis of influencing factors of adverse prognosis of neonatal BPD, and explore the potential application of MALAT1 in it. We will conduct supplementary research based on the above points in the future.

To sum up, MALAT1 can be used as a biomarker for screening and predicting the condition of neonatal BPD. We also proposed for the first time that MALAT1-miR-206 axis can regulate the development of BPD, and clarified its molecular mechanism, which may provide a new treatment direction for neonatal BPD.

## Disclosure of conflict of interest

None.

**Address correspondence to:** Limin Zhang, Neonatal Intensive Care Unit, Zhoukou Central Hospital, No. 26, Renmin East Road, Chuanhui District, Zhoukou 466000, Henan, China. Tel: +86-0394-8269300; E-mail: zhanglimin2005@163.com

## References

[1] Bao TP, Wu R, Cheng HP, Cui XW and Tian ZF. Differential expression of long non-coding RNAs in hyperoxia-induced bronchopulmonary dysplasia. Cell Biochem Funct 2016; 34: 299-309.

[2] Cai C, Qiu J, Qiu G, Chen Y, Song Z, Li J and Gong X. Long non-coding RNA MALAT1 protects preterm infants with bronchopulmonary dysplasia by inhibiting cell apoptosis. BMC Pulm Med 2017; 17: 199.

[3] Abman SH, Bancalari E and Jobe A. The evolution of bronchopulmonary dysplasia after 50 years. Am J Respir Crit Care Med 2017; 195: 421-424.

[4] Sehgal A, Malikiwi A, Paul E, Tan K and Menahem S. A new look at bronchopulmonary dysplasia: postcapillary pathophysiology and cardiac dysfunction. Pulm Circ 2016; 6: 508-515.

[5] Natarajan V, Ha AW, Dong Y, Reddy NM, Ebenezer DL, Kanteti P, Reddy SP, Usha Raj J, Lei Z, Maienschein-Cline M, Arbieva Z and Harijith A. Expression profiling of genes regulated by sphingosine kinase1 signaling in a murine model of hyperoxia induced neonatal bronchopulmonary dysplasia. BMC Genomics 2017; 18: 664.

[6] Savani RC. Modulators of inflammation in bronchopulmonary dysplasia. Semin Perinatol 2018; 42: 459-470.

[7] Fukuhara K, Nakashima T, Abe M, Masuda T, Hamada H, Iwamoto H, Fujitaka K, Kohno N and Hattori N. Suplatast tosilate protects the lung against hyperoxic lung injury by scavenging hydroxyl radicals. Free Radic Biol Med 2017; 106: 1-9.

[8] Ozsurekci Y and Aykac K. Oxidative stress related diseases in newborns. Oxid Med Cell Longev 2016; 2016: 2768365.

[9] Pisoschi AM and Pop A. The role of antioxidants in the chemistry of oxidative stress: a review. Eur J Med Chem 2015; 97: 55-74.
[10] Yangi R, Huang H and Zhou Q. Long noncoding RNA MALAT1 sponges miR-129-5p to regulate the development of bronchopulmonary dysplasia by increasing the expression of HMGB1. J Int Med Res 2020; 48: 300060520918476.
[11] Zhang G, Lan Y, Xie A, Shi J, Zhao H, Xu L, Zhu S, Luo T, Zhao T, Xiao Y and Li X. Comprehensive analysis of long noncoding RNA (lncRNA)-chromatin interactions reveals lncRNA functions dependent on binding diverse regulatory elements. J Biol Chem 2019; 294: 15613-15622.
[12] Mo W, Li Y, Chang W, Luo Y, Mai B and Zhou J. The role of lncRNA H19 in MAPK signaling pathway implicated in the progression of bronchopulmonary dysplasia. Cell Transplant 2020; 29: 963689720918294.
[13] Cui H, Banerjee S, Guo S, Xie N, Ge J, Jiang D, Zornig M, Thannickal VJ and Liu G. Long noncoding RNA Malat1 regulates differential activation of macrophages and response to lung injury. JCI Insight 2019; 4: e124522.
[14] Wang S, Ren L, Shen G, Liu M and Luo J. The knockdown of MALAT1 inhibits the proliferation, invasion and migration of hemangioma endothelial cells by regulating MiR-206/VEGFA axis. Mol Cell Probes 2020; 51: 101540.
[15] Zhang X, Xu J, Wang J, Gortner L, Zhang S, Wei X, Song J, Zhang Y, Li Q and Feng Z. Reduction of microRNA-206 contributes to the development of bronchopulmonary dysplasia through up-regulation of fibronectin 1. PLoS One 2013; 8: e74750.
[16] Lal CV, Olave N, Travers C, Rezonzew G, Dolma K, Simpson A, Halloran B, Aghai Z, Das P, Sharma N, Xu X, Genschmer K, Russell D, Szul T, Yi N, Blalock JE, Gaggar A, Bhandari V and Ambalavanan N. Exosomal microRNA predicts and protects against severe bronchopulmonary dysplasia in extremely premature infants. JCI Insight 2018; 3: e93994
[17] Park MS, Rieger-Fackeldey E, Schanbacher BL, Cook AC, Bauer JA, Rogers LK, Hansen TN, Welty SE and Smith CV. Altered expressions of fibroblast growth factor receptors and alveolarization in neonatal mice exposed to 85% oxygen. Pediatr Res 2007; 62: 652-657.
[18] Maturu P, Wei-Liang Y, Androutsopoulos VP, Jiang W, Wang L, Tsatsakis AM and Couroucli XI. Quercetin attenuates the hyperoxic lung injury in neonatal mice: implications for Bronchopulmonary dysplasia (BPD). Food Chem Toxicol 2018; 114: 23-33.
[19] Chen XQ, Wu SH, Luo YY, Li BJ, Li SJ, Lu HY, Jin R and Sun ZY. Lipoxin A4 attenuates bronchopulmonary dysplasia via upregulation of let-7c and downregulation of TGF-beta1 signaling pathway. Inflammation 2017; 40: 2094-2108.
[20] Jung EY, Park KH, Han BR, Cho SH, Yoo HN and Lee J. Amniotic fluid infection, cytokine levels, and mortality and adverse pulmonary, intestinal, and neurologic outcomes in infants at 32 weeks' gestation or less. J Korean Med Sci 2017; 32: 480-487.
[21] Bi H, Wang G, Li Z, Zhou L, Zhang M, Ye J and Wang Z. Long noncoding RNA (lncRNA) maternally expressed gene 3 (MEG3) participates in chronic obstructive pulmonary disease through regulating human pulmonary microvascular endothelial cell apoptosis. Med Sci Monit 2020; 26: e920793.
[22] Luo F, Wei H, Guo H, Li Y, Feng Y, Bian Q and Wang Y. LncRNA MALAT1, an lncRNA acting via the miR-204/ZEB1 pathway, mediates the EMT induced by organic extract of PM2.5 in lung bronchial epithelial cells. Am J Physiol Lung Cell Mol Physiol 2019; 317: L87-L98.
[23] Tano K, Mizuno R, Okada T, Rakwal R, Shibato J, Masuo Y, Ijiri K and Akimitsu N. MALAT-1 enhances cell motility of lung adenocarcinoma cells by influencing the expression of motility-related genes. FEBS Lett 2010; 584: 4575-4580.
[24] Chen W, Zhao W, Chen S, Zhang L, Guo Z, Wang L, Wang J, Wan Z, Hong Y and Yu L. Expression and correlation of MALAT1 and SOX9 in non-small cell lung cancer. Clin Respir J 2018; 12: 2284-2291.
[25] Lai X, Eberhardt M, Schmitz U and Vera J. Systems biology-based investigation of cooperating microRNAs as monotherapy or adjuvant therapy in cancer. Nucleic Acids Res 2019; 47: 7753-7766.
[26] Tian LJ, Wu YP, Wang D, Zhou ZH, Xue SB, Zhang DY, Wei YG and Liu W. Upregulation of long noncoding RNA (lncRNA) X-inactive specific transcript (XIST) is associated with cisplatin resistance in non-small cell lung cancer (NSCLC) by downregulating microRNA-144-3p. Med Sci Monit 2019; 25: 8095-8104.
[27] Yu X, Zhe Z, Tang B, Li S, Tang L, Wu Y, Chen X and Fang H. alpha-Asarone suppresses the proliferation and migration of ASMCs through targeting the lncRNA-PVT1/miR-203a/E2F3 signal pathway in RSV-infected rats. Acta Biochim Biophys Sin (Shanghai) 2017; 49: 598-608.
[28] Duan J, Zhang X, Zhang S, Hua S and Feng Z. miR-206 inhibits FN1 expression and proliferation and promotes apoptosis of rat type II alveolar epithelial cells. Exp Ther Med 2017; 13: 3203-3208.
[29] Sucre JMS, Jetter CS, Loomans H, Williams J, Plosa EJ, Benjamin JT, Young LR, Kropski JA, Calvi CL, Kook S, Wang P, Gleaves L, Eskaros

A, Goetzl L, Blackwell TS, Guttentag SH and Zijlstra A. Successful establishment of primary type II alveolar epithelium with 3D organotypic coculture. Am J Respir Cell Mol Biol 2018; 59: 158-166.

[30] Zhang Y, Dong X, Shirazi J, Gleghorn JP and Lingappan K. Pulmonary endothelial cells exhibit sexual dimorphism in their response to hyperoxia. Am J Physiol Heart Circ Physiol 2018; 315: H1287-H1292.